IEEE Access
Multidisciplinary | Rapid Review | Open Access Journal

Received June 29, 2018, accepted August 31, 2018, date of publication September 13, 2018, date of current version October 8, 2018.

Digital Object Identifier 10.1109/ACCESS.2018.2869778

Research on a Camera-Based Microscopic Imaging System to Inspect the Surface Luminance of the Micro-LED Array

LILI ZHENG[1], ZIQUAN GUO[1], WEI YAN[1], YUE LIN[1], YIJUN LU[1], HAO-CHUNG KUO[2,3], (Fellow, IEEE), ZHONG CHEN[1], LIHONG ZHU[1], TINGZHU WU[1], AND YULIN GAO[1]

[1]Fujian Engineering Research Center for Solid-State Lighting, Collaborative Innovation Center for Optoelectronic Semiconductors and Efficient Devices, Department of Electronic Science, Xiamen University, Xiamen 361005, China
[2]Institute of Electro-Optical Engineering, National Chiao Tung University, Hsinchu 30010, Taiwan
[3]Optoelectronics Engineering Research Center, Department of Electronic Engineering, Xiamen University, Xiamen 361005, China

Corresponding author: Tingzhu Wu (wutingzhu@xmu.edu.cn) and Yulin Gao (ylgao@xmu.edu.cn)

This work was supported in part by the National Natural Science Foundation of China under Grant 61504112, Grant 11604285, and Grant 51605404, in part by the Technological Innovation Project of Economic and Information Commission of Fujian Province, in part by the Strait Post-Doctoral Foundation of Fujian Province, and in part by the Natural Science Foundation of Fujian Province under Grant 2018J01103.

ABSTRACT A majority of luminance measurement systems are currently focused on measuring the total luminance of light-emitting diodes (LEDs). It has largely limit its application on micro-LEDs, which require capturing the microscopic surface luminance. In order to study the microscopic characteristics of micro-LED displays, in this paper we propose a practical method that can accurately measure the luminance of a whole micro-LED array and even the surface luminance distribution of any single micro-led chip on the array. The essentials of this method are a high-precision complementary metal oxide semiconductor camera and a self-made data processing algorithm. Results show that the maximum error of the luminance measurement is less than 8%, which can prove the accuracy of the method. The metrical wavelength range and the accuracy of system can be dynamically set according to the camera and microscope. Endowed with ultrahigh dynamic ranges, this system proves its competency for evaluating the spatially resolved distribution of luminance for high brightness micro-LEDs.

INDEX TERMS Micro-LED, luminance measurement, microscope with camera, inspection system, 3D luminance distribution.

I. INTRODUCTION

A great deal of research has been focused on the topic of healthy lighting since recent years, because of the high flexibility of spectrum of light-emitting diodes (LEDs) [1]–[3]. If the angular power distribution of a LED chip is not strictly controlled, a blinding glare appears when the chip is viewed from certain angles, and LEDs emit a larger portion of blue lights, compared with conventional light sources [4], it is extremely necessary to quantifiably detect luminance of LEDs, for preventing the dazzling glare as well as reducing the blue-light hazards [5]–[8]. Furthermore, since Jiang *et al.* at Texas Tech University first developed the micro-LED array with chip size of 12 μm and resolution of 10×10 in 2000 [9]. The performance of micro-LED has been improved over the past decade. The resolution of micro-LED display increases from 360 PPI to 1700 PPI [10]–[12], and the design of control system has also been significantly optimized [13]. The team of Kuo in Taiwan successfully applied the Pulsed Spray Coating technology to the UV Micro-LED display screen to achieve the colorization of 35 μm-size microchips, and they optimized the coating process to suppress inter-pixel crosstalk [14]–[17]. However, there is little research on the luminance measurement of micro-LED array, especially on identify the luminance of an individual chip when a micro-LED array is working.

The core of a digital camera is the image sensor, which converts the optical signal to the electrical signal. The analog signal, after undergoing a series of processions, including digitalization by an analog-to-digital converter, is finally stored in the form of image files. These digital signals undergo

further processing via a microprocessor and then are stored in the form of image files. Over the past few years, lots of studies have been done on the use of cameras to obtain luminance [18]–[20]. Hitherto, methods of LED luminance measurement can be roughly divided into the following three categories [21]–[23]. a) Direct measurement by adopting a conventional luminance meter; b) deviating from direct measurements of illuminance, source area, and distance; c) measurement based on a digital imaging photometer.The goal of these traditional method is to identify the average luminance of a large area. This may be suffice for large-size luminance, but when it comes to the micro-LED which requires evaluation of luminance of individual chips, these methods always fail give accurate luminance values from a micron-scale area. However, these shortcomings can be remedied by conducting quantitative spatially-resolved luminance measurements, which provide the luminance-distribution of LED chip or micro-LED array. Therefore, it is urgent to propose a feasible way to quantitatively measure the microscopic surface luminance in real times.

In this study, we propose a method for measuring the spatially-resolved surface luminance of conventional broad-area LED and micro-LED. Acquiring both digital images and camera exposure times, we can accurately and effectively achieve the luminance distribution of each micro-LED chip in the array.

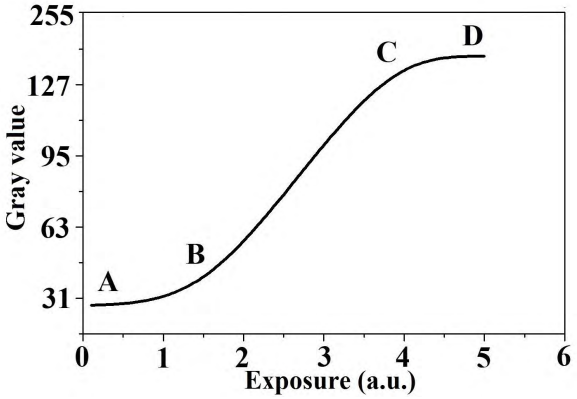

FIGURE 1. A characteristic curve showing the relationship between the level of exposure and the gray value of each pixel on a camera.

II. THEORY AND PRINCIPLE

According to photographic and photometric theories, a camera can take images of an object on the photographic material through lens. The values of each pixels on the image bears a certain relationship with the exposure of the corresponding point of the object. According to the photometrical response function shown in Fig. 1, AB and CD segments on the curve exhibit nonlinearity under insufficient or excessive camera exposures, leading to the blurry of images. To achieve the clarity, we must control the amount of exposure in BC segment. Normally, the brightness degree of the image is measured by using the gray value. The gray value (ranging from 0 to 255) of each pixel position on the image, can be calculated by the following formula [24],

$$D = 0.299R + 0.587G + 0.114B, \tag{1}$$

where D denotes the gray value of the digital image, while R, G and B denote red, green and blue colors of these three channels, respectively.

Under the condition of proper exposure, the gray value of the digital image depends linearly on the logarithm of the exposure, as denoted in (2),

$$D = v \lg H + u, \tag{2}$$

where H denotes the amount of exposure; v denotes the contrast coefficient (the slope of BC segment); and u denotes a constant coefficient.

In (2), H can be defined from the product of illuminance and exposure time,

$$H = Et, \tag{3}$$

where E denotes the illuminance of the imaging plane and t denotes the exposure time of camera.

According to the photometric and geometric optics, we can obtain the following equation,

$$E = \frac{\pi\tau}{4F^2}L, \tag{4}$$

where τ denotes the optical transmission coefficient of lens, F denotes the aperture of camera, and L denotes the actual luminance of planar light source.

With (2-4), we obtain the following equation for the actual luminance as,

$$L = \frac{4}{\pi\tau}\frac{F^2}{t}10^{\left(\frac{D-u}{v}\right)}. \tag{5}$$

To facilitate the calculation, we use a series of polynomials to approximate the Eq. (5). According to Taylors Series Expansion, $f(x) = \frac{f(x_0)}{0!} + \frac{f'(x_0)}{1!}(x-x_0) + \frac{f''(x_0)}{2!}(x-x_0)^2 + \cdots + \frac{f^{(n)}(x_0)}{n!}(x-x_0)^n + R_n(x)$, we can convert $10^{\left(\frac{D-u}{v}\right)}$ to the following equation:

$$10^{\left(\frac{D-u}{v}\right)} = a_0D^0 + a_1D^1 + a_2D^2 + \cdots + a_{n-1}D^{n-1} + a_nD^n, \tag{6}$$

where $a_0, a_1, a_2, ..., a_n$ denote constant coefficients. After omitting the terms beyond the third order, we can obtain the following equation with the aid of (5, 6),

$$L \approx \frac{4}{\pi\tau}\frac{F^2}{t} \times \left(a_3D^3 + a_2D^2 + a_1D^1 + a_0D^0\right). \tag{7}$$

In the case of the specified camera, τ and F are constants if we keep the aperture unchanged. Under this situation, the actual luminance only depends on the exposure time and the gray value of digital image. Consequently, (6) can be converted into,

$$L \approx \frac{lD^3 + mD^2 + nD + a_0}{t}, \tag{8}$$

where l, m, n, and a_0 denote constant coefficients, and t denotes the exposure time.

The actual luminance of LED and the gray value of digital image both vanish when no electrical current flows through the LED chip, yielding the zero value of $a_0 D^0$. Hence, we can obtain the final luminance equation,

$$L = \frac{lD^3 + mD^2 + nD}{t}. \tag{9}$$

Firstly, a proper exposure time is required for capturing a clear digital image. Secondly, we use (1) to calculate the gray value of each pixel position on the image. Finally, we calculate the actual luminance via (9). The advantage of this equation lies in the fact that we can obtain the actual luminance of the LED immediately from the gray value of the digital image and the exposure time.

III. SYSTEM AND VERIFICATION

A. SYSTEM

The system of luminance measurement for micro-LED array includes a computer, electrical current source, digital camera, current supply probe, and microscope, as shown in Fig. 2. A supporting software based on Delphi is developed to control the system and analyze the photomicrograph. And the software includes five function modules such as file handle, camera control, image calibration, measuring tool, and data display.

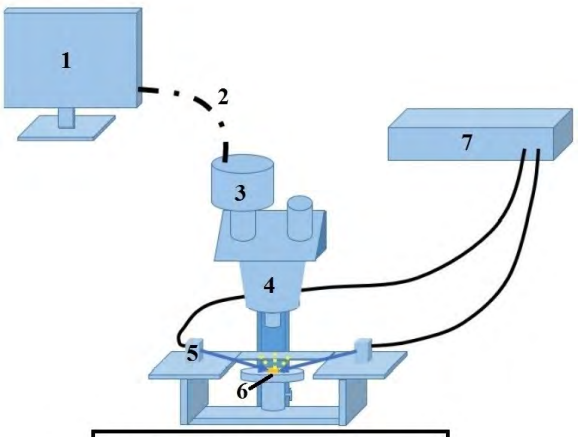

FIGURE 2. The schematic system of microscopic luminance measurement for the micro-LED array.

B. ACQUIREMENT OF LUMINANCE CALIBRATION FILE

The system in Fig. 3(a) aims to obtain the actual luminance by using conventional luminance meter to make a comparison with the measured luminance. The experiment measurement system consists the integrating sphere (500 mm), the LED sources, the electrical current resource (Keithley 2400, Keithley Inc.), the temperature control equipment (Keithley 2510, Keithley Inc.), the optical spectrometer (Spectro 320, Instrument Systems Inc.), the telescopic optical probe (Top 100, Instrument Systems Inc.), the microscope (LED 650C, Everfine Inc.) with the digital camera (MD 50-T, Mshot Inc.), and the computer. The light outlet of integrating sphere has a uniform light distribution. As show in Fig. 3(b), we replace the telescopic optical probe and the spectrometer, with the digital camera and microscope. The camera is controlled to focus on the outlet of the integrating sphere and to capture a clear image at an appropriate exposure time. The detailed parameters of the complementary metal oxide semiconductor (CMOS) camera are shown in the Table 1. The relations between gray value and brightness varies from wavelength of light. Therefore, we adopt a number of commercial blue and green broad-area LEDs in common use. We place the Top 100 in front of the outlet of integrating sphere at a distance of 500 mm, adjust the height of the tripod, and control the Top 100 focus on the outlet. By changing the LED-drive current from 20 mA to 350 mA at 25 °C, we measure corresponding actual luminance of the outlet.

TABLE 1. The parameters of the Mshot camera and lens.

Name	Mshot MD 50-T Scientific Digital Camera
Sensor	1/2.5" CMOS 5.70 mm(H) × 4.28 mm(V) Diagonal 7.13 mm
Effective pixels	2592 H × 1944 V
Pixel size	2.2 μm × 2.2 μm
Scanning method	Progressive Scan
Lens interface	C-mount
Lens focal length	16 mm
Lens aperture value	1.2
Lens image format	1/3"

Then, as shown in Fig. 3(b), we replace the Top 100 with a Mshot digital camera and a LED microscope. Adjusting the camera and LED microscope to focus on the outlet of the integrating sphere, we capture images of outlet at different exposure times and electrical currents (20 mA-350 mA). The images and spectrum of the outlet of the integrating sphere as shown in Fig. 4. The light distribution of the outlet is uniform, so the luminance captured by every pixel can be considered identical. To solve the inhomogeneity of the CMOS pixels in the digital camera to improve the measurement accuracy, it is necessary to conduct the flat field correction of the CMOS in the digital camera. Collected by the digital camera, the image information of the target ($G_I(x, y)$) includes the following three parts. The image information in the exposure time of 0 ($G_O(x, y)$), the image information obtained by changing the exposure time of the digital camera in a dark environment ($G_D(x, y)$), the actual image information of target ($G_A(x, y)$).

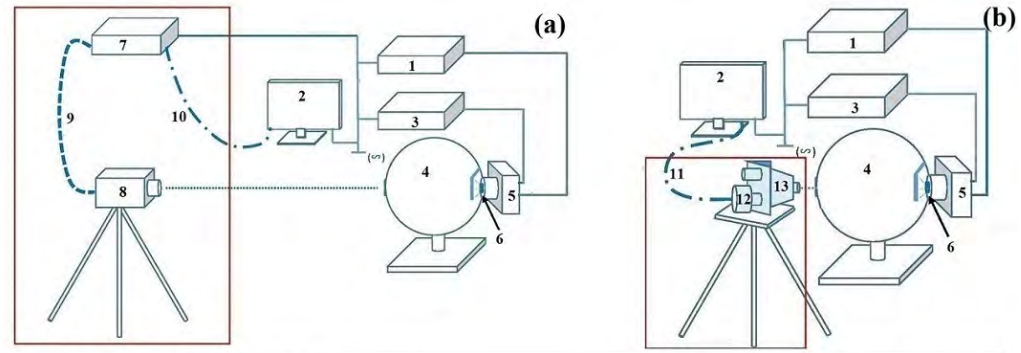

FIGURE 3. The schematic diagram of (a) actual luminance measurement system and (b) image acquisition system.

So the $G_I(x, y)$ can be denoted as,

$$G_I(x, y) = G_O(x, y) + G_D(x, y) + G_A(x, y). \quad (10)$$

For an image of uniform luminance distribution, actual gray values of each pixels should be identical. To prevent the error caused by lens distortion and image black-edge phenomenon, we take the average gray value of 1% of the pixels in the center of the image as the standard gray value (G_S). So the correction coefficient ($Cal(x, y)$) of each pixel in the image captured by the system can be defined as,

$$Cal(x, y) = \frac{G_S - G_O(x, y) - G_D(x, y)}{G_I(x, y) - G_O(x, y) - G_D(x, y)}. \quad (11)$$

So we can obtain a series of two-dimensional matrixes of correction coefficients at different exposure time. To make the calculation more accurate, we must prevent intensities of three channels being saturated, and remove overexposed images at first. We calibrate the gray value of each pixel position on the image according to the correction matrixes, and get the measured gray value D of the image at different exposure time. According to (9), for the image of the LED driven with the same current, the corresponding luminance should be the product of the actual luminance and the exposure time. Therefore, we make a least-square fitting of the gray values of the images of different currents taken at different exposure times and their corresponding luminance values. The result shown in (12, 13), indicating the goodness of our fitting, values of coefficient of determination R^2 exceed 0.999 in this experiment. Equation (14, 15) present the actual luminance of blue and green broad-area LED.

$$\begin{aligned} L_B &= -0.0004D_B^3 + 0.1869D_B^2 + 133.6D_B, \\ R^2 &= 0.99956, \\ L_G &= 0.0036D_G^3 - 0.6262D_G^2 + 153.4D_G, \end{aligned} \quad (12)$$

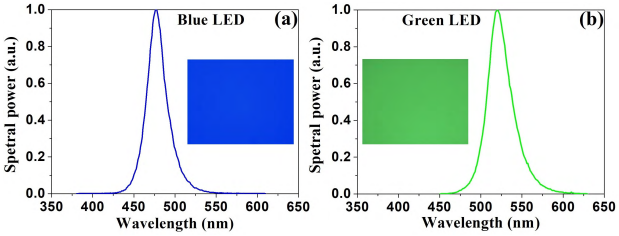

FIGURE 4. The spectrum and the image (insert) of the outlet of the integrating sphere for (a) blue and (b) green broad-area LEDs.

$$R^2 = 0.99902. \quad (13)$$

$$L_B = \frac{-0.0004D_B^3 + 0.1869D_B^2 + 133.6D_B}{t}, \quad (14)$$

$$L_G = \frac{0.0036D_G^3 - 0.6262D_G^2 + 153.4D_G}{t}, \quad (15)$$

C. VERIFICATION

The operation process of the method of luminance measurement for micro-LED array is shown in Fig. 5. First, turn on and initialize the camera, set parameters of the camera and calibrate. Then, take the photomicrograph or import the image for measure. Finally, use the measuring tool to analyze the image.

At exposure time of 1 ms, the original image of the broad-area bare LED captured by our system is shown in the left of Fig. 6, Fig. 6(a) is the image of blue LED driven with 6 mA, and Fig. 6(c) is the image of green LED driven with 7 mA. After the processing of the software, we can plot pseudo color maps presenting the luminance distribution of bare chip in Fig. 6(b) and Fig. 6(d). In those pseudo color maps, green lines are electrodes, blue dots and lines are solder joints and gold wires, respectively. Uneven on surfaces of LED chips,

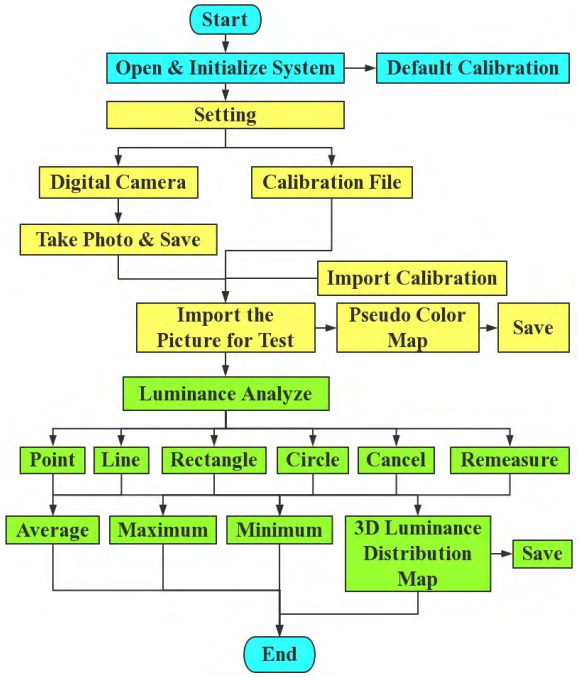

FIGURE 5. The operation process of the method of luminance measurement for micro-LED array.

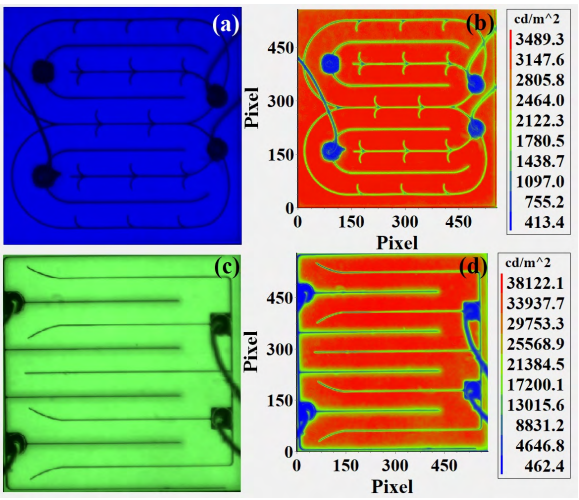

FIGURE 6. The original photomicrograph and the luminance distribution of broad-area LEDs. The (a) is the image of blue LED driven with 6 mA at exposure time of 1 ms and the (c) is the image of green LED driven with 7 mA at exposure time of 1 ms. The (b) and (d) are the pseudo color maps presenting the luminance distribution of blue and green LED, respectively.

luminance of middle portions of chips are high while edge portions are low, according to pseudo color maps.

To evaluate the accuracy of the measurement scheme, a comparison between the results captured by this system is required. Due to the fact that Top 100 can only capture an average luminance of an area, we capture the data from a same region by Top 100 and our system respectively, and average the data from the former and compare it with the latter. We select eight sets of data for error analysis as shown in Table 2. In order to describe the homogeneity of the

TABLE 2. Experimental results of measuring the luminance of blue and green broad-area LEDs.

	Electrical current (mA)	Gray value	U (%)	L_T (cd/m^2)	L_S (cd/m^2)	*Error* (%)
Blue LED	20.0	17	88.2	11200	11740	4.8
	16.0	14	88.5	8901	9585	7.7
	6.0	22	88.0	3049	3188	4.6
	0.9	22	80.9	60.82	62.70	3.1
Green LED	20.0	129	87.7	98580	92570	6.1
	7.0	183	84.5	33074	34083	3.1
	2.5	163	83.2	9546	9082	4.9
	0.07	153	78.7	50.72	48.47	4.4

luminance of the chip surface, we introduce the uniformity factor U, which is defined as the proportion of pixels of which the luminance are within $\pm$ 10% of the average luminance. The luminance measured by Top 100 brightness is denoted as L_T, and the luminance measured by the system is denoted as L_S. In addition, the U and the *Error* in Table 2 is defined as,

$$U = \frac{P_C}{P_T} \times 100\%, \tag{16}$$

$$Error = \frac{|L_S - L_T|}{L_T} \times 100\%, \tag{17}$$

where P_C denotes the the number of the pixels whose luminance are within $\pm$ 10% of the average luminance, and P_T denotes the number of the total pixels in the image. Results show that the maximum error is less than 8%, which can prove the accuracy of our proposed system.

IV. EXPERIMENT AND DISCUSSION

A. EXPERIMENT

We use the system of luminance measurement for micro-LED array to measure the overall light emission of the micro-LED array and the luminance distribution of a single chip. The resolution of micro-LED array used in this experiment is 32 $\times$ 64, and the chip size is 50 μm $\times$ 50 μm, as shown in Fig. 7. In this passive-matrix micro-LED array, when a certain positive and negative electrode are connected to a source, the micro-LED chip at the intersection of the two electrodes will be turned on.

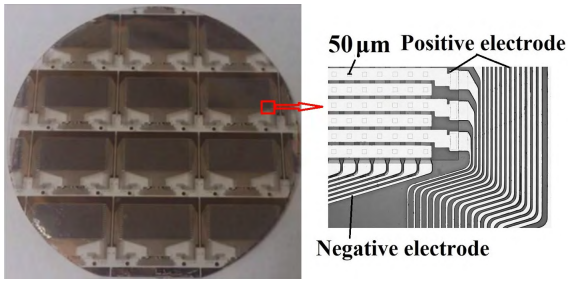

FIGURE 7. The microscopy image of micro-LED arrays on a wafer.

At the beginning, the temperature of the heat sink is controlled at 25 °C. We measure the spatially resolved luminance

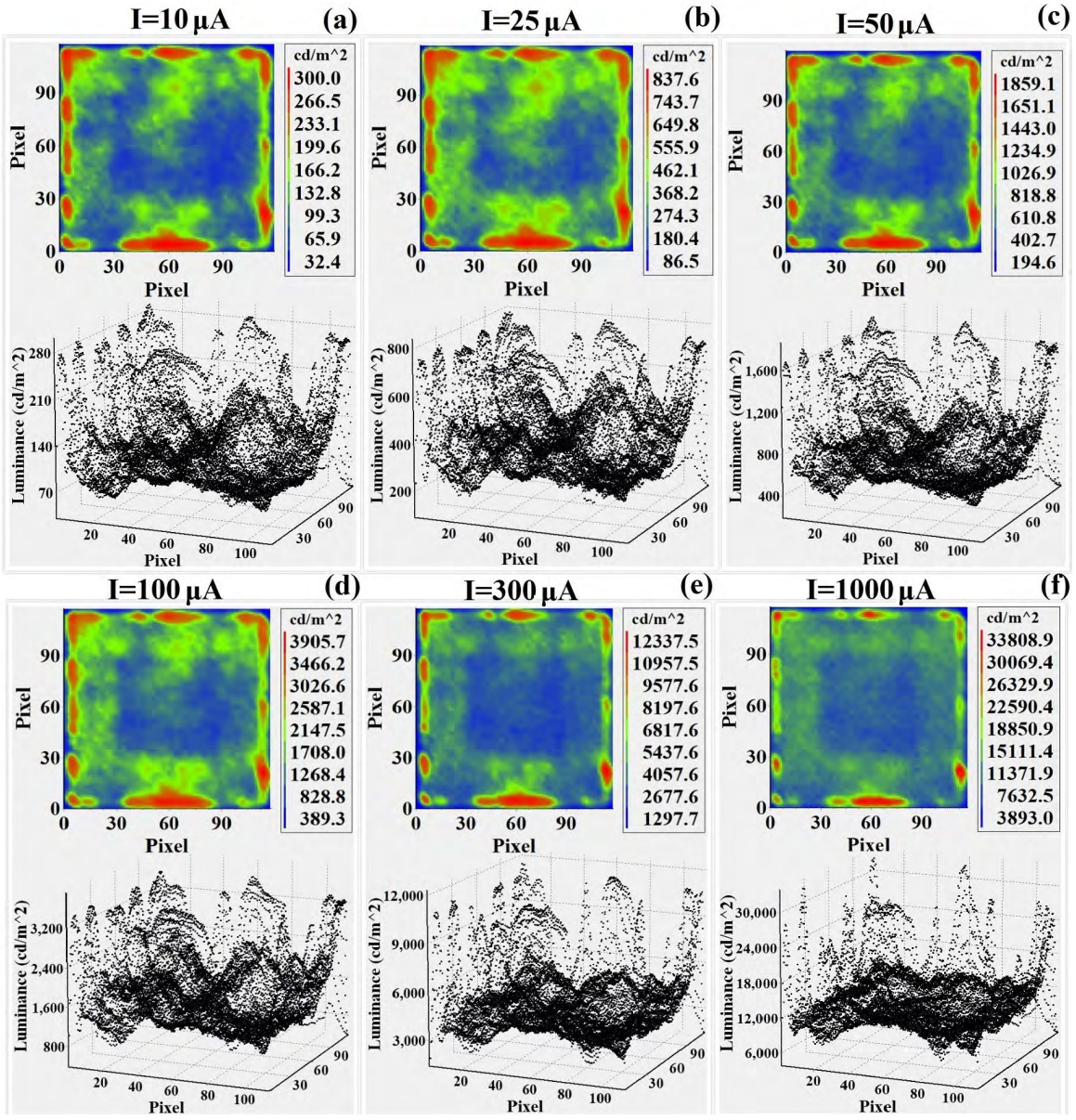

FIGURE 8. The pseudo color map and 3D distribution of the luminance of the single micro-LED chip.

of an individual chip at a series of current, while other chips are all turned off according to the flow chart shown in Fig. 5, and the results are listed in Table 3. The results show that the uniformity of the luminance distribution on the surface of the micro-LED chip increases from 19.7% to 45.4% as the current density increases from 0.4 to 40 A/cm^2. Compared with the broad-area LED chip, the uniformity of micro-LED is much lower because the radiation area primarily located at the edge instead of the middle of the active region [25]. In Fig. 8, we illustrate the pseudo color map and 3D distribution of the luminance of the single micro-LED chip under six different currents. In the 3D chart, we can clearly see that much more points are located near the average luminance with the 1000 uA drive current, which means that large currents can increase the uniformity of the micro-LED chip's surface luminance.

Then we utilize a voltage source to drive all micro-LED chips to measure the average luminance of each single chip because each chip on the passive matrix micro-LED array is connected in parallel. The average luminance of certain chips on micro-LED array at different voltages is shown in Fig. 9. Because the luminance of the No. 8 chip is only about one-third of the remaining chips under the same voltage, we can determine that the No. 8 chip is not working properly. Therefore, our luminance measuring system can quantitatively detect the working status of the micro-LED array, and can also be regarded as a useful tool for practitioners who desire to improve the quality of micro-LED arrays.

TABLE 3. Experimental results of measuring the luminance of the single micro-LED chip.

Electrical current (μA)	Current density (A/cm^2)	Exposure time (ms)	U (%)	Average luminance (cd/m^2)
10	0.4	120	19.7	107
25	1.0	45	22.9	354
50	2.0	20	22.1	687
100	4.0	10	23.7	1558
300	12.0	3	29.7	4068
1000	40.0	1	45.4	11523

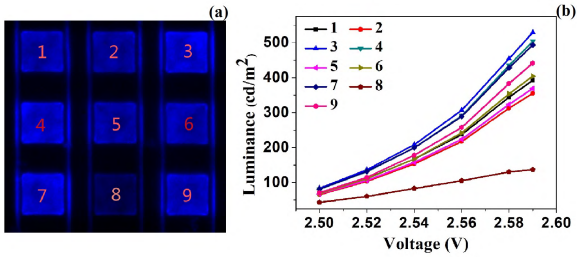

FIGURE 9. (a) The certain chips on the micro-LED array and (b) the average luminance of these chips under different voltages.

B. DISCUSSION

Compared to the previous luminance measurements [20], [23], the method using the camera and microscope for microscopic luminance measurement provides micro-luminance distribution of broad-area LED chip, as well as the actual luminance of each micro-LED chip. This is favorable in at least two cases. The first identifies the crystalline issues including distributions of carrier, dislocation and defect. It reinforces the microscopic-defect detection of semiconductor optoelectronic bulk materials and devices. The second examines the micro-LED display, which is composed of billions of independent, self-emitting microscale chip, arranged in matrices. In this case, the system can check the color uniformity and mark bad micro-LED chips prior to being sold.

V. CONCLUSION

The method measuring the luminance of the micro-LED array based on microscopic imaging system using camera is proposed in this study. The method described above presents following advantages. a) The luminance distribution of each micro-LED chip on the array can be quantitatively measured. b) With the image of a micro-LED array and the exposure time of the camera, we can obtain the actual luminance of a single chip when the whole micro-LED array is working. c) In comparison to conventional luminance measurements, the proposed method yields higher measurement efficiencies.

REFERENCES

[1] M. H. Crawford, "LEDs for solid-state lighting: Performance challenges and recent advances," *IEEE J. Sel. Topics Quantum Electron.*, vol. 15, no. 4, pp. 1028–1040, Jul./Aug. 2009.

[2] L. L. Zheng *et al.*, "Spectral optimization of three-primary LEDs by considering the circadian action factor," *IEEE Photon. J.*, vol. 8, no. 6, Dec. 2016, Art. no. 8200209.

[3] T. Wu *et al.*, "Multi-function indoor light sources based on light-emitting diodes—A solution for healthy lighting," *Opt. Express*, vol. 24, no. 21, pp. 24401–24412, Oct. 2016. [Online]. Available: http://www.opticsexpress.org/abstract.cfm?URI=oe-24-21-24401

[4] Y.-M. Shang, G.-S. Wang, D. Sliney, C.-H. Yang, and L.-L. Lee, "White light–emitting diodes (LEDs) at domestic lighting levels and retinal injury in a rat model," *Environ. Health Perspect.*, vol. 122, no. 3, pp. 269–276, 2014.

[5] T. Wu *et al.*, "Improvements of mesopic luminance for light-emitting-diode-based outdoor light sources via tuning scotopic/photopic ratios," *Opt. Express*, vol. 25, no. 5, pp. 4887–4897, 2017.

[6] M. Rózanowska, J. Jarvis-Evans, W. Korytowski, M. E. Boulton, J. M. Burke, and T. Sarna, "Blue light-induced reactivity of retinal age pigment *in vitro* generation of oxygen-reactive species," *J. Biol. Chem.*, vol. 35, no. 32, pp. 18825–18830, 1995.

[7] Y.-S. Chen, C.-Y. Lin, C.-M. Yeh, C.-T. Kuo, C.-W. Hsu, and H.-C. Wang, "Anti-glare LED lamps with adjustable illumination light field," *Opt. Express*, vol. 22, no. 5, pp. 5183–5195, 2014.

[8] P. Liu *et al.*, "Uniform illumination design by configuration of LEDs and optimization of LED lens for large-scale color-mixing applications," *Appl. Opt.*, vol. 52, no. 17, pp. 3998–4005, 2013.

[9] S. X. Jin, J. Li, J. Z. Li, J. Y. Lin, and H. X. Jiang, "GaN microdisk light emitting diodes," *Appl. Phys. Lett.*, vol. 76, no. 5, pp. 631–633, 2000.

[10] Z. J. Liu, W. C. Chong, K. M. Wong, and K. M. Lau, "360 PPI flip-chip mounted active matrix addressable light emitting diode on silicon (LEDoS) micro-displays," *J. Display Technol.*, vol. 9, no. 8, pp. 678–682, 2013.

[11] Z. J. Liu, W. C. Chong, K. M. Wong, K. H. Tam, and K. M. Lau, "A novel BLU-free full-color LED projector using LED on silicon micro-displays," *IEEE Photon. Technol. Lett.*, vol. 25, no. 23, pp. 2267–2270, Dec. 1, 2013.

[12] W. C. Chong, W. K. Cho, Z. J. Liu, C. H. Wang, and K. M. Lau, "1700 pixels per inch (PPI) passive-matrix micro-LED display powered by ASIC," in *Proc. IEEE Compound Semiconductor Integr. Circuit Symp. (CSICs)*, Oct. 2014, pp. 1–4.

[13] K. Zhang, D. Peng, K. M. Lau, and Z. Liu, "25-5: *Distinguished student paper*: Fully-integrated active matrix programmable UV and blue micro-LED display system-on-panel (SoP)," in *SID Symp. Dig. Tech. Papers*, 2017, vol. 48, no. 1, pp. 357–361.

[14] H.-V. Han *et al.*, "Resonant-enhanced full-color emission of quantum-dot-based micro LED display technology," *Opt. Express*, vol. 23, no. 25, pp. 32504–32515, 2015.

[15] H.-Y. Lin *et al.*, "Optical cross-talk reduction in a quantum-dot-based full-color micro-light-emitting-diode display by a lithographic-fabricated photoresist mold," *Photon. Res.*, vol. 5, no. 5, pp. 411–416, 2017.

[16] S.-C. Hsu *et al.*, "Fabrication of a highly stable white light-emitting diode with multiple-layer colloidal quantum dots," *IEEE J. Sel. Topics Quantum Electron.*, vol. 23, no. 5, Sep./Oct. 2017, Art. no. 2000409.

[17] C. W. Sher *et al.*, "A high quality liquid-type quantum dot white light-emitting diode," *Nanoscale*, vol. 8, no. 2, pp. 1117–1122, 2018.

[18] F. M. Martínez-Verdú, J. Pujol, M. Vilaseca, and P. Capilla, "Reproduction model with luminance adaptation for digital cameras," in *Proc. Conf. Colour Graph., Imag., Vis. (CGIV)*, 2002, pp. 529–533.

[19] N. Hashimoto, M. Sato, Y. Takahashi, M. Kasuga, and M. Sato, "Luminance correction with raw digital images," in *Proc. ACM SIGGRAPH Res. Posters*, 2006, p. 71, doi: 10.1145/1179622.1179705.

[20] D. Wüller and H. Gabele, "The usage of digital cameras as luminance meters," *Proc. SPIE*, vol. 6502, p. 65020U, Feb. 2007.

[21] U. Krüger and F. Schmidt, "The impact of cooling on CCD-based camera systems in the field of image luminance measuring devices," *Metrologia*, vol. 46, no. 4, p. S252, 2009.

[22] D. R. Agaphonov, V. S. Ivanov, V. I. Sapritsky, and R. I. Stolyarevskaya, "Light measurements of high-luminance LEDs," *Metrologia*, vol. 37, no. 5, p. 587, 2000.

[23] Y. Tyukhova and C. Waters, "An assessment of high dynamic range luminance measurements with LED lighting," *Leukos*, vol. 10, no. 2, pp. 87–99, 2014.

[24] Q. Ruan, *The Study of Digital Image Processing*. Electronic Industry Press, 2013.

[25] F. Olivier, S. Tirano, L. Dupré, B. Aventurier, C. Largeron, and F. Templier, "Influence of size-reduction on the performances of GaN-based micro-LEDs for display application," *J. Lumin.*, vol. 191, pp. 112–116, Nov. 2017. [Online]. Available: http://www.sciencedirect.com/science/article/pii/S0022231316308547

LILI ZHENG received the B.S. and M.S. degrees from the Department of Electronic Science, Xiamen University, Xiamen, China, in 2014 and 2017, respectively, where she is currently pursuing the Ph.D. degree with the Department of Electronic Science.

ZIQUAN GUO received the Ph.D. degree from Xiamen University, Xiamen, China, in 2014. He is currently an Engineer with the Department of Electronic Science, Xiamen University.

WEI YAN received the B.S. and M.S. degree from the Department of Electronic Science, Xiamen University, Xiamen, China, in 2014 and 2017, respectively. He is currently with Xiamen University.

YUE LIN received the Ph.D. degree from Xiamen University, Xiamen, China, in 2012. He is currently an Associate Professor with the Department of Electronic Science, Xiamen University.

YIJUN LU received the Ph.D. degree from Xiamen University, Xiamen, China, in 2000. He is currently a Professor with the Department of Electronic Science, Xiamen University.

HAO-CHUNG KUO received the B.S. degree in physics from National Taiwan University, Taipei, Taiwan, the M.S. degree in electrical and computer engineering from Rutgers University, New Brunswick, NJ, USA, in 1995, and the Ph.D. degree from the University of Illinois at Urbana–Champaign, Champaign, IL, USA, in 1999. He is currently the Associate Dean of the Office of International Affair, National Taiwan University.

ZHONG CHEN received the Ph.D. degree from Xiamen University, Xiamen, China, in 1993. He is currently a Professor with the Department of Electronic Science, Xiamen University.

LIHONG ZHU received the Ph.D. degree from Xiamen University, Xiamen, China, in 2010. She is currently a Senior Engineer with the Department of Electronic Science, Xiamen University.

TINGZHU WU received the Ph.D. degree from Xiamen University, Xiamen, China, in 2017. He is currently a Post-Doctoral Fellow with the Department of Electronic Science, Xiamen University.

YULIN GAO received the Ph.D. degree from Xiamen University, Xiamen, China, in 2002. Since 2011, she has been with the Department of Electronic Science, Xiamen University, where she is currently an Associate Professor.